

UC Riverside

UC Riverside Previously Published Works

Title

Optimizing Security Systems with an Optimum Design of a Hybrid Renewable Energy System

Permalink

<https://escholarship.org/uc/item/9v4313k6>

Journal

Electric Power Components and Systems, ahead-of-print(ahead-of-print)

ISSN

1532-5008

Authors

Kiyak, Mahmut Hidayi
Purlu, Mikail
Turkay, Belgin Emre
[et al.](#)

Publication Date

2023

DOI

10.1080/15325008.2023.2251477

Copyright Information

This work is made available under the terms of a Creative Commons Attribution License, available at <https://creativecommons.org/licenses/by/4.0/>

Peer reviewed



Optimizing Security Systems with an Optimum Design of a Hybrid Renewable Energy System

Mahmut Hudayi Kiyak,^{1,2} Mikail Purlu,³ Belgin Emre Turkey,¹ and Tahir Cetin Akinci^{1,4}

¹Department of Electrical Engineering, Istanbul Technical University, Istanbul, Turkiye

²ASELSAN Inc, Ankara, Turkiye

³Department of Electrical and Electronic Engineering, Sivas Cumhuriyet University, Sivas, Turkiye

⁴Winston Chung Global Energy Center, University of California at Riverside (UCR), Riverside, CA, USA

CONTENTS

1. Introduction
 2. Simulation Data
 3. Case Studies
 4. Optimization Results of the Security System
 5. Discussion of Results
 6. Conclusion
- References

Abstract—Security systems play a crucial role in protecting individuals and assets within diverse infrastructures, including seaports. The uninterrupted operation of these systems heavily relies on a continuous power supply, as any disruptions can lead to severe consequences. Therefore, security systems are classified as critical loads requiring uninterrupted power availability. This study focuses on the investigation of an optimal hybrid energy system (HES) to ensure a reliable power supply for security systems in two seaports located in Turkiye. Through the utilization of the HOMER software, optimization analyses were conducted, considering both conventional sources such as grid-generator or grid-generator-battery configurations, as well as off-grid and on-grid HES solutions integrating photovoltaic (PV) and wind turbine technologies. The findings reveal that on-grid HES solutions incorporating PV and wind technologies offer a more cost-effective and dependable energy supply for security systems in seaports, surpassing traditional alternatives. This study represents a significant contribution to the existing literature, as it presents the first comprehensive optimization study on the design of HES for security systems. The outcomes serve as a valuable reference for future research endeavors in this field.

1. INTRODUCTION

Enhancing security measures and safeguarding individuals and valuable assets are paramount concerns in today's world. This is particularly crucial in high-risk locations, including seaports, energy plants, and country borders, where continuous surveillance and protection are imperative. To address these challenges, security systems have been implemented to ensure security in critical areas and structures, by deterring potential threats and promptly addressing security issues. Security systems are integral components of critical areas and structures, and any disruption to their operation can lead to severe consequences.

Keywords: security, renewable energy, hybrid power systems, wind energy, solar energy, solar radiation, energy storage, storage batteries

Received 7 August 2023; accepted 20 August 2023

Address correspondence to Tahir Cetin Akinci. E-mail: tahircetin.akinci@ucr.edu

ABBREVIATIONS

ATM	Automated Teller Machine	NASA	National Aeronautics and Space Administration
CO	Carbon Monoxide	NPC	Net Present Cost
CO ₂	Carbon Dioxide	O&M	Operating & Maintenance Cost
COE	Cost of Energy	PV	Photovoltaic
CT	Converter	POWER	Prediction of Worldwide Energy Resource – NASA
EPDK	Turkiye Energy Market Regulatory Authority	RE	Renewable Energy
HES	Hybrid Energy System	RES	Renewable Energy System
HOMER	Hybrid Optimization Models for Energy Resources	RR	Renewable Rate
IC	Initial Investment Cost	WT	Wind Turbine
IT	Information Technologies		
MGM	Turkish Meteorology General Directorate		

Consequently, ensuring an uninterrupted power supply to these security systems is of utmost importance.

This study focuses on proposing hybrid energy system (HES) solutions specifically tailored for security systems in the Samsun and Antalya seaports in Turkiye. By leveraging HES, which combines multiple energy sources, this research aims to optimize the energy supply to security systems, ensuring their continuous operation and resilience. The findings of this study contribute to the advancement of security system infrastructure and provide valuable insights for enhancing the security measures in seaport environments.

Renewable energy systems (RES) face sustainability issues owing to geographical, meteorological, and technological limitations, despite their potential for environmentally friendly energy production. HES with multiple sources has become increasingly important for addressing these issues. HES can provide uninterrupted energy by using other sources when the RE source is insufficient. Energy storage units in HES can store energy produced during high production periods and provide a reliable energy source for low production periods. In addition, previous studies have shown that on-grid HES solutions can reduce energy costs.

The aim of this study is to determine the most suitable optimized HES solution that provides uninterrupted energy while considering technical, economic, and emission factors and specified limitations. The Hybrid Optimization Models for Energy Resources (HOMER) software was used for optimization studies, and four different scenarios were presented, including off-grid and on-grid HES options with PV and wind turbine options in addition to grid-generator or grid-generator-battery sources typically preferred in security systems. This study evaluated 31 different sub-case studies using grid, generator, battery, PV, and wind turbine (WT) options for the two regions. Case studies with different energy sources were compared economically,

the effects of geographic factors on the system design were examined, and sensitivity analyses were conducted to investigate the effects of the selected energy sources on the system. In addition, this paper presents the most comprehensive optimization study to date for HES for security systems.

A. Literature Review

Previous studies have examined HES optimization for various target areas, such as villages, campuses, data centers, and ATMs, with the use of HOMER software being common among these studies. In this literature review, we have examined the following studies:

Arina, Razak, and Othman conducted an optimization study using the HOMER software for a region in Southern Malaysia in 2010. They determined that a system with a WT, generator, and battery configuration is the most suitable solution [1]. Turkay and Telli analyzed the optimum HES solution with grid, hydrogen, PV, and WT source options for the Electrical and Electronics Faculty of Istanbul Technical University, in Turkiye, using the HOMER software in 2011. They revealed that the on-grid HES solution is the most suitable [2]. In 2013, Sharma, Singh, and Khemariya carried out an optimization study using HOMER software for HES consisting of PV, WT, generator, and battery units for a base station located in the Imalaya region of India, which is currently powered by diesel generator [3]. In 2013, Iverson, Achuthan, Marzocca, and Aidun developed an uninterrupted and low-cost HES optimization algorithm for data centers with PV, WT, and hydrogen sources [4]. Okedu and Uhumwangho performed optimization for two different off-grid HES structures using the HOMER software in 2014 and examined the effects of variable load profiles on the results [5].

In 2016, Magarappanavar and Sreedhar analyzed an off-grid HES solution for the Bapatla Engineering College (BEC) Campus in India, including PV, WT, battery, and diesel generator resources, using the HOMER software [6]. Baneshi and Hadianfard analyzed on-grid and off-grid HES systems, including PV, WT, and battery systems, for the Shiraz region in southern Iran using the HOMER software in 2016 [7]. In 2016, Swarnkar, Sharma, and Gidwani carried out an optimization study using the HOMER software for an on-grid HES including PV, WT, generator, and battery units for the Rajasthan Technical University campus in Kota, India [8]. Nurunnabi and Roy conducted an optimization study with HOMER for on-grid and off-grid HES solutions including PV, WT, and batteries for a rural area in Bangladesh in 2016 [9]. Kumar et al. simulated and optimized HES solution consisting of PV, WT, and diesel generator units in HOMER software for an ATM located in Kolhapur, India in 2016 [10]. Bahramara, Moghaddam, and Haghifam performed optimization studies using the HOMER software for 91 different regions and load profiles worldwide in 2016 [11].

Halabi et al., compared the actual data with the HOMER software results for the HES with PV, generator, and battery configurations installed in Sabah, Malaysia in 2017 [12]. Mas'ud carried out optimization work on the HOMER software for the off-grid HES solution, which includes PV, WT, and battery units, for the Nigerian state of Sokoto in 2017 [13]. Jamalaliah et al., carried out simulation and optimization work using HOMER software for HES solution covering PV, hydrogen, and battery units for a base station located in Kolkata, India in 2017 [14]. In 2017, Yeshalem and Khan conducted analyses for an off-grid HES using the HOMER software for a base station located in the Ethiopian Oromia region, powered by diesel generator and battery groups [15].

In 2018, Grange et al., introduced a new approach for data centers, including RES, and analyzed an on-grid HES with PV units [16]. Nurunnabi et al., performed optimization and sensitivity analyses in HOMER software with 4 different source configurations for 5 different regions of Bangladesh in 2019 [17]. In 2019, Azad et al., presented an off-grid HES solution consisting of PV, WT, gas turbine, and battery units for the Rohingya Relocation Center in Bangladesh [18]. Cetinbas et al., carried out an optimization application using HOMER software for the HES solution, which included PV, generator, and battery units, for the Eskisehir Osmangazi University Health Complex in Turkiye in 2019 [19]. Usman et al., used HOMER software for the design and simulation of on-grid and off-grid HES

with diesel generator for telecommunication sites located in the Kashmir region of Pakistan in 2019 [20].

Khalil et al., performed optimization for the Balochistan coastal region in 2020 using HOMER software for on-grid HES with PV and WT [21]. In 2020, Kwon developed a mathematical optimization model that included PV and battery units to use RES, increase energy efficiency, and reduce energy costs in data centers with variable power consumption [22]. Kumaran et al., conducted feasibility analyses with the HOMER program for hybrid RES for the Indian Institute of Education in 2021 [23]. Purlu, Beyarslan, and Turkey worked on a microgrid design with HES solution for a village located in Bursa, Turkiye in 2021 [24]. Sawle et al., conducted an analysis and design study using the HOMER program for an off-grid HES solution for a rural area in Gujarat, India, in 2021 [25]. Uwineza, Kim, and Ki Kim performed HES solution analysis and optimization, which included PV, WT, generator, and battery units, for Popova Island in 2021 using the Monte Carlo model and HOMER software [26]. Sharma et al., carried out the analysis and optimization studies in HOMER software for HES solution consisting of bioenergy, PV, and battery units for a village in India in 2021 [27]. Kabir et al., conducted an optimization study using HOMER software for off-grid HES, which includes PV, WT, generator, and battery units, using the load profiles determined for the green data center concept in 2021 [28]. Sitanggang conducted feasibility analyses for HES in 2022 using the HOMER software for the Water Island region in Indonesia, which was energized for a limited time [29]. Sawhney et al., conducted feasibility analyzes of a microgrid using HOMER software for a campus in Savona, Italy, in 2022 [30]. Al Badi and Al Wahaibi proposed a hybrid RES using HOMER software for Al-Mazyouna province in Oman in 2022 [31].

B. Paper Organization

The rest of the paper is organized as follows. Section II provides general information about the data and components used in the simulation and analysis studies. Section III presents a summary of the scenarios considered in the simulations and analyses. Section IV shares the simulation and analysis results. Section V presents a discussion of the results. Finally, the conclusions are presented.

2. SIMULATION DATA

This study employed the HOMER software for conducting an analysis, optimization, and sensitivity analysis of hybrid

energy system (HES) solutions for security system load profiles. It encompasses general information about the study regions, simulation data, and unit costs. The objective is to identify the most suitable HES solution for uninterrupted power supply to security systems in selected regions, considering regional disparities, while ensuring cost-effectiveness and environmental sustainability.

A. Regions Selected in Simulation Studies

In this study, two seaports in Türkiye with different climatic conditions were selected. The Long Years (2004-2021) Average Global Solar Radiation Map of Türkiye [32] and Wind Map of Türkiye [33] shared by the Turkish Meteorology General Directorate (MGM) are shown in Figures 1 and 2, respectively. Based on these maps, it is possible to make a general assessment of the solar

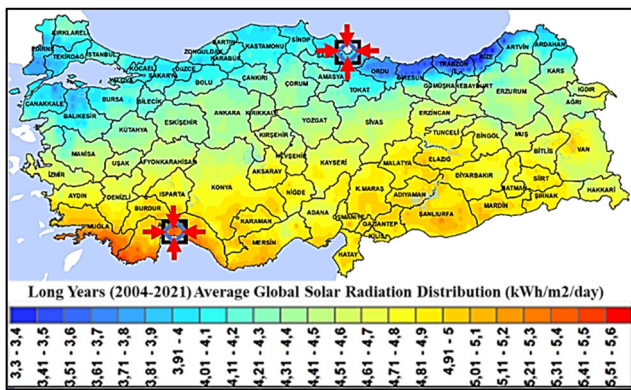


FIGURE 1. Representation of the locations on the solar radiation map of Türkiye.

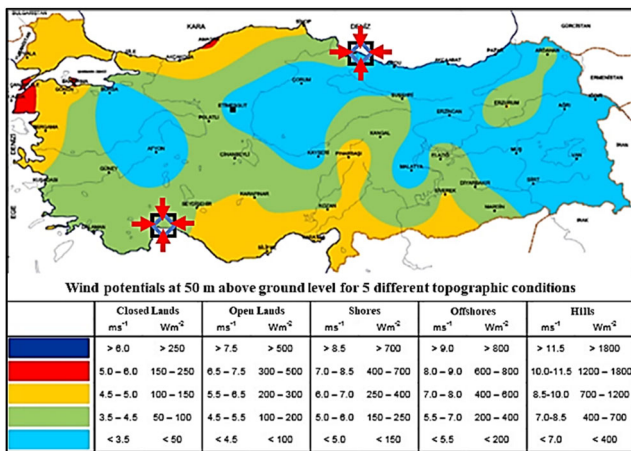


FIGURE 2. Representation of the locations on the wind map of Türkiye.

radiation conditions and wind potentials of the regions throughout Türkiye.

The solar radiation map shows that the southern regions have more solar radiation potential than the northern regions. When evaluating the wind potential of the regions, it is seen that there is generally low wind potential in the eastern regions, and the region with the highest potential is located around Canakkale in the northwest.

Considering these data, the provinces of Samsun (Region-1) and Antalya (Region-2), which have different wind and solar radiation values, were chosen as study regions. Table 1 lists the selected regions and their coordinates. The locations of these regions on the map are shown in Figures 3 and 4.

B. Load Profile

Security systems play a crucial role in critical facilities and areas that carry security risks. Failure or malfunction of these systems can lead to serious consequences, such as loss of life, property damage, and even terrorist attacks. Therefore, these systems are considered to be critical loads and require an uninterrupted power supply. They typically exhibit constant power consumption and 24/7 operating loads. In this study, the same security system load profile was used for both the regions. The subsystems included in

Region	Selected region	Coordinates
Region-1	Samsun Seaport	41°18'03.6"N – 36°20'02.4"E
Region-2	Antalya Seaport	36°50'07.8"N – 30°36'11.8"E

TABLE 1. Regions selected in simulation studies.

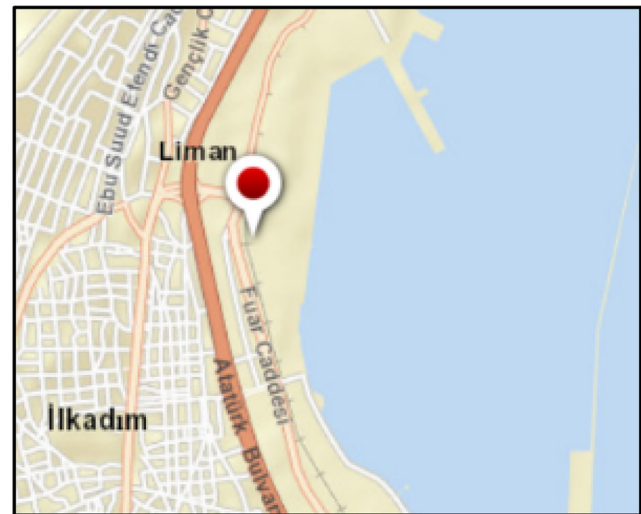


FIGURE 3. Map location of Region-1.

the load profile are as follows:

- CCTV Cameras
- Detection Sensors (fiber optic, radar, etc.)
- Network Devices
- Converters
- Network Recording Devices
- Servers
- Monitoring Computers and Monitors
- Monitoring Screens
- Lighting
- Air Conditioning System
- Fire Alarm and Extinguishing System

The use of air conditioning varies depending on the climate conditions, lighting usage, and opening-closing operations of various sensors (such as cameras) during day-night cycles also cause minor fluctuations in load consumption. The security system has an average

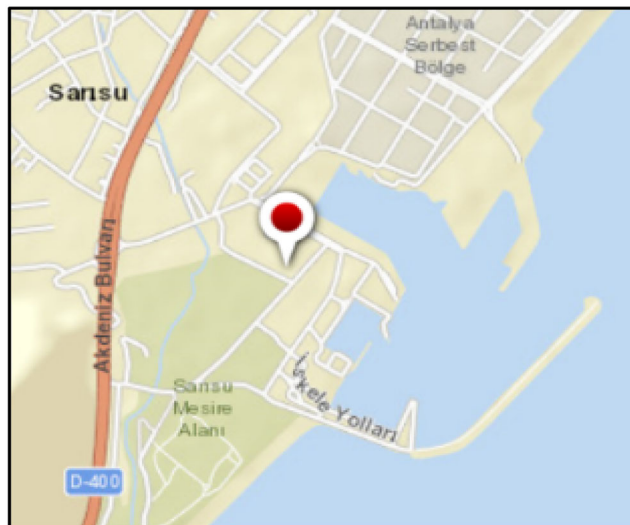


FIGURE 4. Map location of Region-2.

instantaneous power consumption of 30 kW AC, peak load of 35 kW, and load factor of 85%. Detailed data and graphs for the load profile were obtained using the HOMER software and are presented in Figures 5 and 6.

C. Design Constraints

Six different constraints are considered in the simulations. Analyses were conducted while adhering to the determined constraints.

- The first constraint concerns the life expectancy of the system, with the aim of designing a system that can function for 25 years.
- The second constraint is related to the interruption rate of the output power, with the security system equipment being considered critical priority loads, with the aim of finding a solution that avoids interruptions.
- The third constraint involves planned grid outages, with the 9-hour power outage event that occurred throughout Turkey in 2015 due to maintenance of the mainlines serving as a reference [34]. It is assumed that there will be four regular 9-hour planned interruptions every year in March, June, September, and December owing to maintenance, failures, etc.
- The fourth constraint concerns the grid purchase-sale power limit. In the on-grid HES solution, the grid purchase side was assumed to be 20 kW and 35 kW power limits, and the grid sales side was assumed to have power limit of 0, 10, and 20 kW.
- The fifth constraint pertains to the installation area limits for the PV, WT, and batteries. A maximum of 200 PV panels and a maximum of 20 m high WT will be allowed to be installed, and there is enough area to install a maximum of 100 Li-ion batteries with a capacity of 1 kW.
- The sixth and final constraints were related to the upper power limit of the generator. In the grid-generator-battery system solutions, it is assumed that the

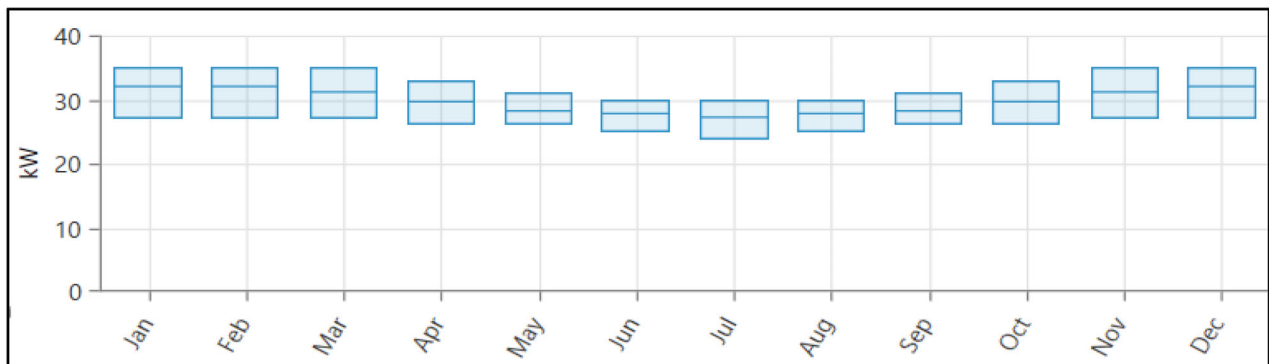


FIGURE 5. Monthly load profile of security system.

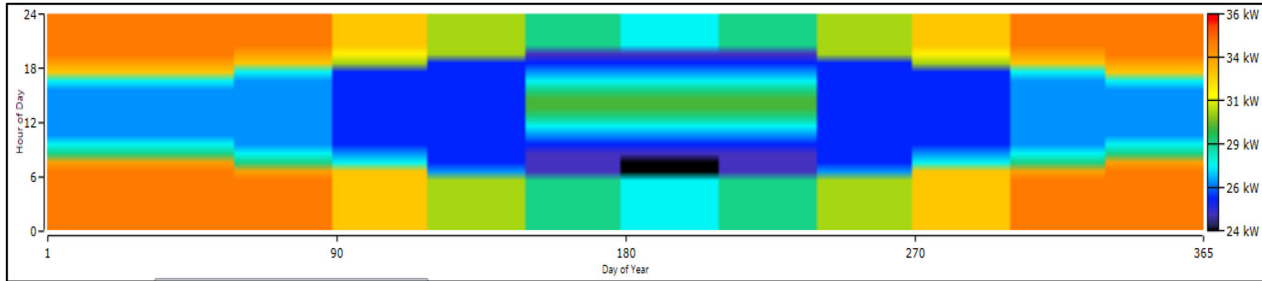


FIGURE 6. Yearly load profile of security system.

Month	REGION-1		REGION-2	
	Clearness index	Daily radiation (kWh/m ² /day)	Clearness Index	Daily radiation (kWh/m ² /day)
Jan	0.418	1.680	0.438	2.090
Feb	0.446	2.420	0.470	2.880
Mar	0.459	3.420	0.515	4.120
Apr	0.457	4.350	0.520	5.120
May	0.485	5.330	0.553	6.130
Jun	0.538	6.240	0.620	7.170
July	0.559	6.300	0.636	7.180
Aug	0.549	5.520	0.615	6.320
Sep	0.527	4.290	0.615	5.300
Oct	0.470	2.830	0.568	3.790
Nov	0.435	1.880	0.509	2.580
Dec	0.395	1.420	0.424	1.850

TABLE 2. Solar radiation data for regions.

diesel generator capacity options will reach a maximum of 10 kW and 20 kW, respectively.

D. Solar Radiation Data in Regions

The solar radiation and clearness index data were subjected to rigorous analysis using the HOMER software and the NASA POWER database for a specific region of interest. The collected dataset, consisting of monthly average daily radiation values, underwent meticulous collection and processing procedures. The clearness index, which ranged between 0 and 1, was employed as a quantitative parameter to assess the extent of cloud cover. A clearness index value of 0 indicated complete overcast conditions, while a value of 1 represented entirely clear skies. The corresponding values extracted from the NASA POWER database for the two specified regions are meticulously documented in Table 2. This comprehensive investigation provides a scientifically grounded comprehension of solar radiation patterns and the clearness index, thereby enabling accurate assessments of energy resources and the exploration of potential solar applications in the examined regions.

E. Wind Potential Data in Regions

Wind potential analyses were conducted using wind speed data obtained using HOMER software from the NASA POWER database for the selected region. The data are presented as monthly average wind speed values. Table 3 presents the wind-speed data for the two regions. Accurate wind speed data are crucial for the proper design and optimization of wind energy systems.

F. Energy Purchase and Sale Prices

The study utilized energy cost data sourced from the Turkiye Energy Market Regulatory Authority (EPDK), the regulatory body responsible for overseeing energy prices. The EPDK data, subject to periodic updates, were employed in this research, with electricity prices from October 2022 and diesel fuel prices from November 2022 considered. Table 4 provides a comprehensive summary of these prices, contributing to a comprehensive analysis of the energy cost landscape in the study.

G. Equipment Used in Simulation

In this section, we provide details of the components preferred by HOMER software for simulation and analysis studies.

1) *Diesel Generator.* A general diesel generator model available in the HOMER library was selected for simulation. Details of the diesel generator model are presented in Table 5.

In the grid-generator-battery system solutions, fixed power values of 15 kW and 20 kW were employed. The output power-fuel consumption data for the 40 kW diesel generator are presented in Table 6, offering a detailed overview of the relationship between power output and fuel consumption in the system.

Month	Average wind speed for Region-1 (m/s)	Average wind speed for Region-2 (m/s)
Jan	5.590	4.640
Feb	5.380	4.670
Mar	4.620	4.020
Apr	3.830	3.350
May	3.350	2.920
Jun	3.540	3.300
July	4.060	3.480
Aug	4.000	3.210
Sep	3.800	3.230
Oct	4.070	3.480
Nov	4.900	3.900
Dec	5.640	4.540

TABLE 3. Wind speed data for regions.

Energy type	Purchase price	Sale price
Grid Electricity	0.19 \$/kWh	0.02 \$/kWh
Diesel Fuel	1.33 \$/L	–

TABLE 4. Electricity and diesel fuel unit costs.

2) *Battery*. In this study, 48 V Li-ion type battery packs with a 1kWh energy capacity were selected as the preferred choice due to their widespread availability in the market. Table 7 provides a comprehensive overview of the specifications and details of these batteries, offering valuable insights into their characteristics, performance parameters, and other relevant information.

3) *PV Panel*. In this study, the X21-335-BLK PV panel model from SunPower in the HOMER library was used for analysis. The details of the PV panels are presented in Table 8.

4) *Wind Turbines*. In this study, a comprehensive analysis and optimization were performed on two different wind turbine (WT) models, with a maximum height constraint of 20 m, to determine the optimal solution. The detailed specifications and characteristics of the WT models are presented in Table 9, enabling a thorough understanding of their technical attributes and performance parameters. This investigation provides valuable insights for selecting the most suitable WT model, taking into account the height limitation and considering various factors such as efficiency, power output, and other relevant characteristics.

Parameters	Values
Rated Capacity: (Depends on results)	0 – 40 kW
Minimum Load Rate:	25 %
Capital Cost:	500 \$/kW
Replacement Cost:	500 \$/kW
Operating Cost:	0.3 \$/op.hr.
Minimum Run Time:	0 min.
Lifetime:	15,000 hr.

TABLE 5. Diesel generator parameters.

Output power (kW)	Fuel consumption (L/hr)
0	1.370
5	2.735
10	4.100
15	5.465
20	6.830
25	8.195
30	9.560
35	10.925
40	12.290

TABLE 6. Generator output power and fuel consumption.

Parameters	Values
Nominal Voltage:	48 V
Nominal Capacity:	1 kW
Initial State of Charge:	100 %
Minimum State of Charge:	25 %
Maximum Quantity:	100
Capital Cost:	857 \$/kWh
Replacement Cost:	857 \$/kWh
Operating and Maintenance Cost:	10 \$/kWh
Number Of Cycle:	3000
Lifetime:	15 years

TABLE 7. Li-ion battery parameters.

The relationship between the output power and wind speed for both selected WT models is presented in Table 10.

5) *Converter*. For the simulation, a specific general converter (CT) model from the HOMER library was chosen. The selected CT model offers a range of functionalities and specifications suitable for the study’s requirements. A comprehensive overview of the CT model, including its technical details and characteristics, is presented in Table 11. The details provided in the table serve as valuable information for understanding the capabilities and performance parameters of the CT model employed in the simulation. By utilizing this particular CT model, the study aims to

Parameters	Values
Brand:	SunPower
Model:	X21-335-BLK
Nominal Capacity:	335 W
Panel Efficiency:	21 %
Derating Factor:	88 %
Ground Reflection Ratio:	20 %
Temperature Effect:	-0.3 %/°C
Maximum Quantity:	200
Capital Cost:	765 \$/kW
Replacement Cost:	765 \$/kW
Operating and Maintenance Cost:	10 \$/kW
Lifetime:	25 years

TABLE 8. Li-ion battery parameters.

Parameters	Values
WT-1 Brand:	Eocycle
WT-1 Model:	EO10
WT-1 Power Capacity:	10kW
WT-1 Hub Height:	16 meters
WT-2 Brand:	AWS
WT-2 Model:	HC 5.1 kW
WT-2 Power Capacity:	5.1 kW
WT-2 Hub Height:	12 meters
Capital Cost:	1354 \$/kW
Replacement Cost:	1354 \$/kW
Operating and Maintenance Cost:	22 \$/kW
Lifetime:	20 years

TABLE 9. Wind turbines parameters.

Eocycle EO10 (WT-1)		AWS HC 5.1kW (WT-2)	
Wind speed (m/s)	Output power (kW)	Wind speed (m/s)	Output power (kW)
2.75	0.0200	2.20	0.0619
3.00	0.4000	2.70	0.1402
3.50	1.2000	3.10	0.2235
4.00	2.4000	3.60	0.3447
4.50	3.7000	4.00	0.4722
5.00	5.5000	4.50	0.6237
5.50	7.5000	4.90	0.8321
6.00	11.5000	5.40	1.1162
6.50	11.5000	5.80	1.2727
7.00	11.5000	6.30	1.4722
7.50	11.5000	6.70	1.6376
8.00	11.5000	7.10	1.8106
		7.60	2.0480
		8.00	2.1616

TABLE 10. Wind turbines output power.

accurately assess and optimize the performance of the hybrid renewable energy system under investigation.

6) *Grid*. In the on-grid analysis scenarios, the energy cost for purchasing from the grid was set at 0.19 \$/kWh, while the selling price of energy to the grid was assumed to be 0.02 \$/kWh. Standard emission values provided by HOMER were utilized for the grid-side emissions. To replicate real-world conditions, the study incorporated 9-h grid interruptions on the 21st day of March, June, September, and December, which coincide with the longest day and longest night of the year. These interruptions were accounted for due to potential malfunctions or scheduled maintenance. Regular grid outages were scheduled between 09:00 and 17:00 to enhance the demand for renewable energy sources.

3. CASE STUDIES

In this study, four main solution scenarios were identified: on-grid generator, on-grid generator and battery, off-grid hybrid energy system (HES), and on-grid HES incorporating generator-battery-photovoltaic (PV)-wind turbine (WT) resource options. Based on these resource options, a total of 31 distinct sub-case studies were developed, considering factors such as generator capacity, WT alternatives, grid power limits for purchase and sale, and different operating regions. The detailed specifications of these scenarios are presented in Table 12.

For Scenario 3, four sub-case analyses were carried out, considering two different operating regions and two distinct WT options. In the case of Scenario 4, a total of 24 sub-case analyses were conducted, incorporating two different operating regions, two WT options, and six variations of grid power limits for purchase and sale. Consequently, a total of 31 sub-case analyses were conducted across all scenarios, allowing for a comprehensive exploration of

Parameters	Values
Unit Capacity:	1 kW
Efficiency:	95 %
Capacity Utilization:	100 %
Maximum Quantity:	Depends on results
Capital Cost:	750 \$/kW
Replacement Cost:	750 \$/kW
Operating and Maintenance Cost:	30 \$/kW
Lifetime:	15 years

TABLE 11. Converter parameters.

various configurations and parameters within the study's scope.

4. OPTIMIZATION RESULTS OF THE SECURITY SYSTEM

In this section, the simulation results obtained using HOMER software for each determined scenario are presented. The optimum solutions were examined using 31 case studies for the four main scenarios. The most suitable solutions among the four scenarios are determined and compared. Sensitivity analyses were performed by making changes up to 25% in fuel cost, solar radiation, and wind speed parameters. Results are presented for each study region.

H. On-Grid Generator Solution

In Scenario-1, the optimal solution was presented with the electrical grid and generator source options. There are no restrictions on grid usage and generator power. The system block diagram created using the HOMER software is shown in Figure 7.

Using the specified energy source options, the HOMER software calculated a single solution result. According to this result, the generator usage was 25 kW. Because no RE source was used, the renewable rate was calculated to be 0%. The selected component sizes for the analyzed energy system and cost analyses of Scenario-1 are given in Table 13. The unit COE of Scenario-1 is 0.1937 \$/kWh. This value is above the grid purchase costs of 0.19 \$/kWh.

A large part of the Net Present Cost (NPC) of the system is due to the use of the grid. When viewed proportionally, 97.7% of the NPC was the energy cost incurred from

the grid. generator operates actively only during planned grid outages. There is a 9-h working situation in 3-month periods for the generator unit during the year. While only 0.34% of the annual energy required by the security system is provided by the generator, 99.7% is fully supplied from the grid. The generator usage rate is negligible when considering general energy usage. When the emission values were examined, the energy system released 165,277 kg of CO₂ and 4,5 kg of CO annually. The use of fossil fuels negatively affects emissions values, which is inevitable.

I. On-Grid Generator and Battery Solution

In Scenario-2, the Li-ion battery option was added to the source options, in addition to the electricity grid and generator. The optimal solution was obtained using the source options in the HOMER software. No usage constraints are imposed on the electricity grid. However, to evaluate the effectiveness of battery usage, the generator usage was limited to 15 kW and 20 kW. The battery was limited to 100 units, as specified by the general constraints. The system block diagram created using HOMER software is presented in Figure 8.

Using the determined energy source options, analyses were conducted using HOMER software with two separate generator limits of 15 and 20 kW. The results of these analyses are presented in Table 14. Because no RES were used, the renewable energy rate was calculated to be 0%. In both solutions, the determined upper limits of the generator were fully utilized. When the analysis results were examined, it was observed that the unit COE was 0.226 \$/kWh for the 15 kW generator limit and 0.202 \$/kWh for the 20 kW generator limit. Although both values exceeded the grid purchase cost of 0.19 \$/kWh, the solution with a

Case No.	Sub-case	Energy resource configuration	Gen capacity limit	Grid purchase power Limit	Sales to grid power limit
1	1	Grid-Generator	—	—	0 kW
2	2.1	Grid-Generator	15 kW	—	0 kW
	2.2	-CT-Battery	20 kW	—	0 kW
3	3	Generator -CT-Battery-PV-WT (Off-Grid HES)	—	N/A	N/A
4	4.1	Grid-Generator	—	20 kW	0 kW
	4.2	-CT-Battery-PV-		20 kW	10 kW
	4.3	WT (On-		20 kW	20 kW
	4.4	Grid HES)		35 kW	0 kW
	4.5			35 kW	10 kW
	4.6			35 kW	20 kW

TABLE 12. Case studies.

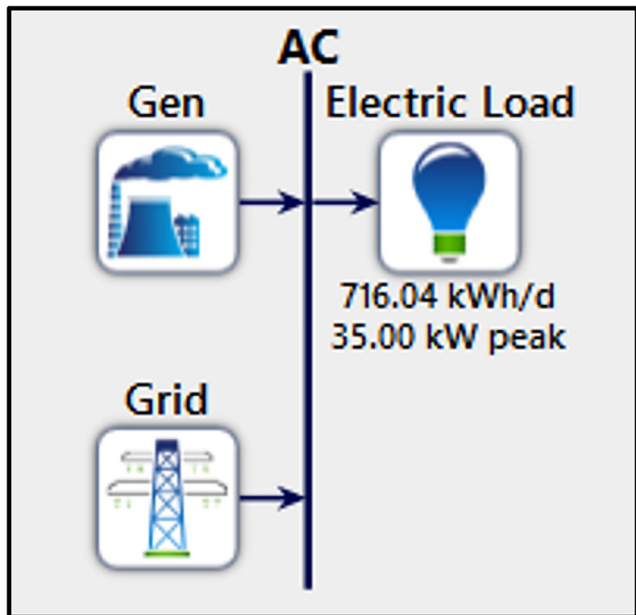


FIGURE 7. System block diagram for Scenario 1.

generator limit of 20kW appears to be more economical. At the same time, the scenario with a 15kW generator limit, which has less generator usage, can be considered more environmentally friendly.

The 15kW generator-limited solution showed more favorable emission values. However, when the unit COE, IC, O&M, and NPC values were evaluated, the most economical solution for Scenario-2 was the 20kW generator-limited solution.

It has been observed that a significant portion of the costs incurred in the 20kW generator-limited solution is for energy purchased from the grid. When examined proportionally, 93.9% of the NPC value was the cost of energy obtained from the grid, while the generator usage rate in NPC was 1.8%, and the battery and CT usage rates were 4.4%.

In the 20kW generator-limited solution, only 0.29% of the annual energy demand of the security system was provided by the generator. In total, 99.7% of the annual energy demand was fully met by the grid. The generator usage rate was insignificant in terms of general use.

Considering the high degree of criticality, the analyses were conducted to achieve an outage rate of 0%. The analysis revealed that 0.08% of the energy demanded by the load cannot be met annually. It is observed that the percentage of electricity demand that cannot be met increases compared to the Scenario 1 solution. However, excessive energy production was not observed.

Case	Energy Resource Options	System Component Size						System Costs					
		Gen. Usage Upper Limit	Gen. (kW)	Bat. (UNIT)	CT (kW)	PV (kW)	WT1 (UNIT)	WT2 (UNIT)	RR (%)	NPC Yrs- (\$)	COE (\$/kWh)	O&M (\$/yr)	IC (\$)
1	Grid-Gen	—	25	—	—	—	—	—	0%	\$654,305	\$0.1937	\$49,646	\$12,500

TABLE 13. Simulation results of Scenario-1.

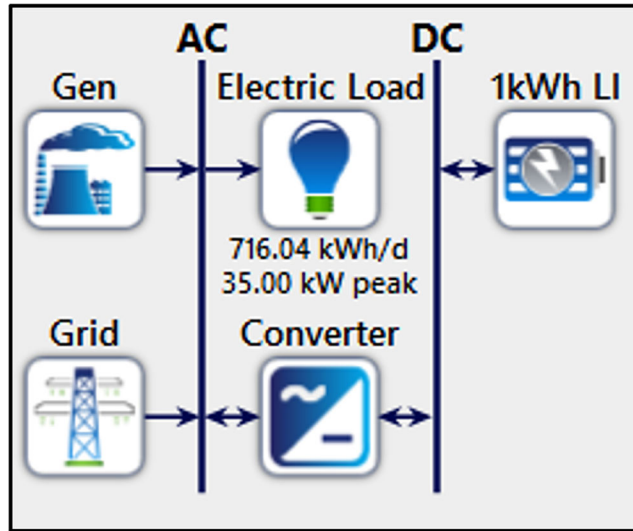


FIGURE 8. System block diagram for Scenario 2.

When the emission values were analyzed, the energy system emitted 165,188 kg of CO₂ and 3.86 kg of CO annually. It is understood that Scenario-2 solutions are more environmentally friendly than the Scenario-1 solution.

J. Off-Grid Hybrid Energy System Solutions

In Scenario-3, the optimal off-grid HES solution was presented using the generator, battery, PV, and WT components. Analyses were conducted using two alternative WT models. The first alternative model was EO10, whereas the second alternative model was AWS 5.1 kW. Optimization studies were conducted separately for the four different case studies for each study region. No limit was applied for generator usage, whereas PV usage was limited to 200 units (134 kW), battery usage was limited to 100 units, and WT usage was limited to one unit.

The analysis studies conducted with the first WT alternative EO10 are described as Scenario 3.1 for Region-1 and Scenario 3.2 for Region-2. The analysis studies with the second WT alternative, AWS 5.1 kW, are described as Scenario 3.3 for Region-1 and Scenario 3.4 for Region-2. A system block diagram from HOMER software for these scenarios is shown in Figure 9.

Analyses were conducted for off-grid HES for security systems located in two different geographical regions, and the results are presented in Table 15. The analyses showed that all planned components were included in the optimum solutions.

Upon examining the costs obtained from the analyses, it can be seen that the unit COE was 0.3546 \$/kWh in Scenario-3.1, 0.3543 \$/kWh in Scenario-3.2, 0.3846 \$/kWh

Case	Sub-case	Energy resource options	System component size										System costs				
			Gen. usage upper limit	Gen. (kW)	Bat. (UNIT)	CT (kW)	PV (kW)	WT1 (UNIT)	WT2 (UNIT)	RR (%)	Yrs- (\$)	NPC -25 (\$)	COE (\$/kWh)	O&M (\$/yr)	IC (\$)		
2	2.1	Grid-	15kW	15	82	12.8	—	—	—	—	—	0%	\$762,303	\$0.226	\$52,795	\$79,798	
	2.2	Gen-Bat	20kW	20	17	7.18	—	—	—	—	—	0%	\$681,475	\$0.202	\$50,519	\$28,388	

TABLE 14. Simulation results of Scenario-2.

in Scenario-3.3 and 0.3732 \$/kWh in Scenario-3.3. Although these values are well above the grid purchase cost of 0.19 \$/kWh, Scenario-3.1 and Scenario-3.2 using the first WT alternative appear to be more economical. The results obtained for Scenario-3.1 and Scenario-3.2 can be considered more environmentally friendly because of the high use of RE. It was determined that the off-grid HES solution identified for Region-2 was more economical than Region-1. This is because Region-2 is located further south and can utilize the PV panels more efficiently. However, the IC for Scenario-3.2 is high.

Upon evaluating the unit COE, IC, O&M, NPC, and environmental impacts, it was determined that the most cost-effective and environmentally friendly solutions in Scenario-3 were Scenario-3.1 and Scenario-3.2 with the first WT alternative being used.

- The details of the Scenario-3.1 solution identified as the optimal off-grid HES solution for Region-1 are as follows.

The analysis reveals that a large portion of the expenses for Scenario-3.1 is attributable to the use of generator, which accounts for 82.7% of the NPC. PV usage contributed 10.2%, WT 1.5%, and battery and CT usage 5.8% to NPC.

In the system solution devised for Scenario-3.1, 47.2% of the annual energy demand of the security system was supplied by the PV, 42% by the generator, and 10.8% by the WT. Although the usage of the generator is high, 58% of the required energy can be obtained from RE sources.

The analysis indicates that during the summer months, most of the energy demand was met by the PV panels, whereas the

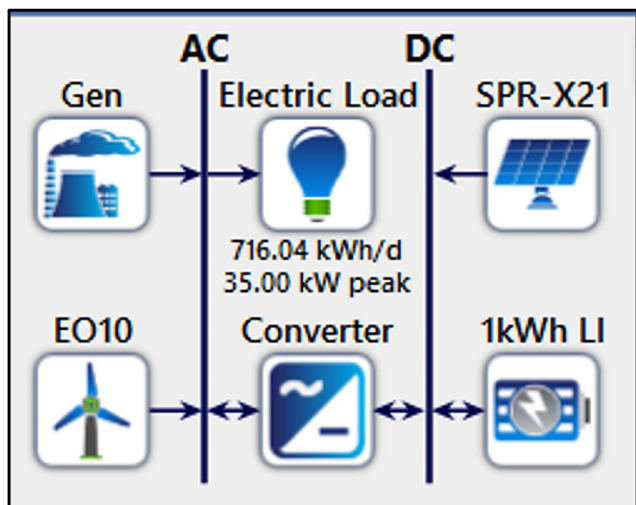


FIGURE 9. System block diagram of Scenario-3.

Case	Sub-case	Energy resource options	System component size						System Costs					
			Region	Gen. (kW)	Bat. (UNIT)	CT (kW)	PV (kW)	WT1 (UNIT)	WT2 (UNIT)	RR (%)	NPC -25 yrs- (\$)	COE (\$/kWh)	O&M (\$/yr)	IC (\$)
3	3.1	Gen-Bat-	Region-1	35	19	31.6	124	1	—	42.1%	\$1,198,083	\$0.3546	\$79,084	\$175,720
	3.2	PV-WT1	Region-2	35	22	31.6	127	1	—	41.7%	\$1,197,034	\$0.3543	\$78,645	\$180,350
	3.3	Gen-Bat-	Region-1	35	31	31.5	133	—	1	34.7%	\$1,299,310	\$0.3846	\$86,749	\$177,866
	3.4	PV-WT2	Region-2	35	22	31.5	130	—	1	36.8%	\$1,260,783	\$0.3732	\$83,868	\$176,584

TABLE 15. Simulation results of Scenario-3.

usage of the generator was minimal. As energy production from PV panels declines during winter months, this shortfall is covered by the use of generator. Wind energy usage increased during the summer months. The analysis concludes that the energy demand for the load is fully satisfied throughout the year in Region-1, and the optimal solution reveals the potential for excess energy production.

The system generates 125.020 kg of CO₂ and 780 kg of CO annually. In terms of CO emissions, the results of Scenario-3.1 are more favorable than those of Scenario-1 and Scenario-2.

- The details of the Scenario-3.2 solution identified as the optimal off-grid HES solution for Region-2 are as follows:

A significant portion of the investment cost for Scenario-3.2 is attributed to the use of generator, accounting for 81.7% of the NPC. In comparison, the contribution of PV panel usage to the NPC was 10.5%, whereas the contributions of the WT, battery, and CT usage were 6.3% and 1.5%, respectively.

In the system solution for Scenario-3.2, 52.6% of the annual energy demand for the security system was supplied by the PV panels, 40.2% by the generator unit, and 7.19% by the WT. When the usage of the generator is high, 59.79% of the energy demand can be fulfilled by the RE sources. Compared with the Scenario-3.1 result for Region-1, it can be concluded that the system in Region-2 is more efficient in terms of RE generation.

The analysis revealed that the majority of the energy needs during the summer months were met by PV panels, whereas generator usage was low. As the energy produced by the PV panels decreases during the winter months, the gap is bridged by the use of generator, and the energy obtained from wind increases during the summer months. The production profile in this state is similar to Scenario-3.1. The analysis indicated that the energy demand throughout the year is met entirely by the load, and the optimum solution offers the potential for excess energy production.

When examining the emission values, it was found that the energy system in Region-2 produces 124,678 kg of CO₂ and 778 kg of CO annually. In terms of CO emissions, the results were more favorable than those of Scenario-1 and Scenario-2. Compared with Scenario-3.1, it yielded better emission results.

K. On-Grid Hybrid Energy System Solutions

In Scenario-4, optimal on-grid HES solutions were proposed by utilizing a combination of resource options,

including the generator, battery, PV, and WT, supported by the grid. Similar in Scenario-3, two alternative WT models were used. For Scenario-4, case studies were generated with varying grid purchase and sales power limits. A total of 24 case studies were analyzed, with 12 for each region. The grid purchase limits were set at 20 and 35 kW, and the grid sale limits were set at 0, 10, and 20 kW.

No limit was applied for generator usage, but PV panel usage was restricted to 200 units (134 kW), battery usage was limited to 100 units, and WT usage was limited to one unit. A system block diagram from HOMER software for these scenarios is shown in Figure 10.

Analyses were conducted for on-grid HES for security systems located in two different geographical regions, and the results are presented in Table 16. Simulation results were obtained for 24 different subcases with two different WT options and six different grid purchase/sale power limits for Region-1 and Region-2.

As the grid purchase power limit increases, the need for generator disappears in the optimal solutions. Similar results were obtained for scenarios with 35 kW/10 kW and 35 kW/20 kW grid purchase/sales power limits. This is because grid sales are not advantageous in terms of known costs. However, in terms of high sales potential, the results with EO10 and AWS 5.1 kW WTs used and the grid purchase/sale power limit set to 35 kW/20 kW were the best results in Scenario 4. These are Scenario-4.21 and Scenario-4.23 for Region-1, and Scenario-4.22 and Scenario-4.24 for Region-2.

Upon examining the costs obtained from the analyses, it can be seen that the unit COE was 0.1522 \$/kWh in Scenario-4.21, 0.1537 \$/kWh in Scenario-4.22, 0.1706 \$/kWh in Scenario-4.23 and 0.1660 \$/kWh in Scenario-4.24. These values were below the grid purchase costs of 0.19 \$/kWh. However, the results obtained with the first WT alternative were more economical. The results obtained for Scenario-4.21 and Scenario-4.22 can be considered more environmentally friendly than other solutions owing to the high use of RE.

The results showed that costs can be reduced as grid purchase and sale capacities increase. When the results are evaluated in terms of the unit COE, IC, O&M, NPC, and environmental effects, it is evident that scenario solutions that utilize the first WT alternative and have the highest grid purchase/sale capacities are the most economical and environmentally friendly. These solutions are Scenario-4.21 for Region-1 and Scenario-4.22 for Region-2.

- The details of the Scenario-4.21 solution identified as the optimal on-grid HES solution for Region-1 are as follows:

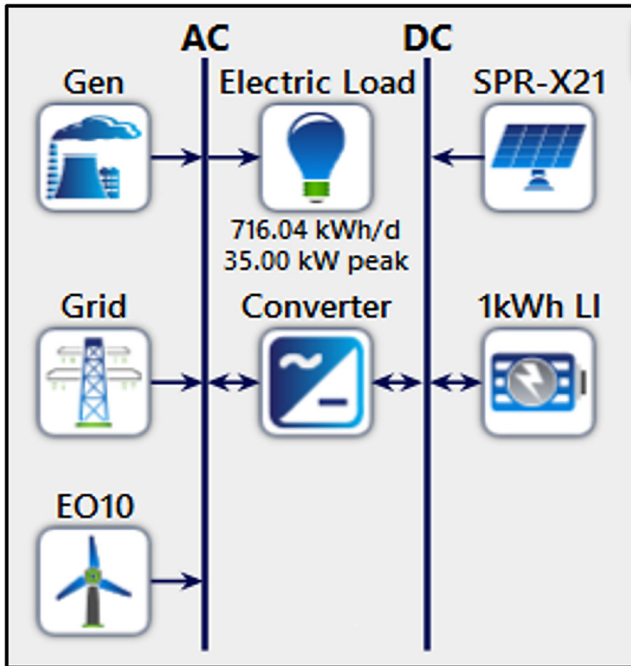


FIGURE 10. System block diagram of Scenario-4.

A significant proportion of the costs incurred in Scenario 4.21 were due to grid usage, accounting for 78.6% of the NPC. The contribution of PV panel usage to NPC was 10.7%, that of WT was 3.5%, and that of battery and CT usage was 7.2%.

In the system solution obtained for Scenario 4.21, 27.4% of the annual energy required by the security system was met by the PV panels, 13.6% by the WT, and 59.1% by the grid. Although the grid usage rate was high, 41% of the energy required could still be obtained from RE sources.

Throughout the year, the majority of energy needs are met by the grid. However, PV panels contributed more to the system during the summer months, whereas WT contribution increased during the winter months. The analysis confirms that the energy demanded by the load throughout the year is fully satisfied, and the determined optimum solution reveals an energy production potential above the requirement.

When analyzing the emission values, it was observed that the energy system releases 106,561 kg of CO₂ annually, and because there is no generator use, CO emissions are absent.

A comparison of the results with Scenario-1, Scenario-2, and Scenario-3 confirms that the proposed on-grid hybrid system is highly environmentally friendly in terms of CO emissions. Compared to Scenario-4.22, it yielded

better emission results.

- The details of the Scenario-4.22 solution identified as the optimal on-grid HES solution for Region-2 are as follows:

A significant proportion of the costs incurred in Scenario-4.22 is attributed to grid usage, accounting for 77.2% of the NPC. PV panel usage constituted 11.4% of NPC, whereas WT, battery, and CT usage contributed 3.4% and 7.6%, respectively.

The system solution for Scenario-4.22 meets 33% of the annual energy required by the security system from PV panels, 9.31% from the WT, and 57.7% from the grid. Although the grid usage rate was high, 42.3% of the energy required could still be obtained from renewable energy sources. Compared to the Scenario-4.21 result of Region-1, it can be concluded that the system in Region-2 is more efficient in terms of RE generation.

Throughout the year, the majority of energy needs are met by the grid, with PV panels contributing more in the summer months and less in the winter months. Conversely, WT's contribution to the system increased during winter months. The analysis showed that energy demand was fully met throughout the year. The determined optimal solution indicates the potential for energy production above the demand.

In terms of emission values, the proposed energy system releases 106,753 kg of CO₂ annually, with no CO emissions, because there generator is not used. Comparing Scenario-1, Scenario-2, and Scenario-3, it is evident that the proposed on-grid hybrid system solution is environmentally friendly with respect to CO emissions.

L. Sensitivity Analysis

Sensitivity analyses were conducted for the optimum solutions obtained for the four main scenarios by examining the effects of the various parameters on the results. Specifically, sensitivity analyses were performed for a 25% decrease in fuel cost, a 25% increase in solar radiation, and a 25% increase in wind speed. These sensitivity analyses allowed for a better understanding of how the system performance would be affected by changes in these important parameters. As part of the sensitivity analysis, the effects of the relevant parameters on the unit COE and renewable rate were examined in detail for each region, as presented below.

1) *General Evaluation for Region-1.* Figure 11 presents comparisons of the unit COE obtained for Region-1 through sensitivity analyses, which are specific to each scenario. Bar graphs are presented for each scenario,

Case	Sub-case	Energy resource options	Grid purchase /Sale limits	Region	System component size							System costs				
					Gen. (kW)	Bat. (UNIT)	CT (kW)	PV (kW)	WT1 (UNIT)	WT2 (UNIT)	RR (%)	NPC -25 Yrs- (\$)	COE (\$/kWh)	O&M (\$/yr)	IC (\$)	
4	4.1	Grid-Gen-Bat-PV- WT1	20kW / 0kW	Region-1	15	9	24.7	67	1	—	—	36.6%	\$720,547	\$0.2133	\$47,701	\$103,894
	4.2	Grid-Gen-Bat-PV- WT2	20kW / 0kW	Region-2	15	9	26.1	67.8	1	—	—	36.1%	\$740,566	\$0.2192	\$49,113	\$105,652
	4.3	Grid-Gen-Bat-PV- WT2	20kW / 0kW	Region-1	15	10	27.3	78.2	—	—	—	29.3%	\$819,367	\$0.2425	\$54,910	\$109,517
	4.4	Grid-Gen-Bat-PV- WT1	20kW / 10kW	Region-2	15	9	27.6	77.8	—	—	—	31.6%	\$801,097	\$0.2371	\$53,563	\$108,660
	4.5	Grid-Gen-Bat-PV- WT1	20kW / 10kW	Region-1	15	8	24.9	67.1	1	—	—	38.4%	\$718,850	\$0.2073	\$47,612	\$103,349
	4.5	Grid-Gen-Bat-PV- WT2	20kW / 10kW	Region-2	15	9	26.1	67.4	1	—	—	37.6%	\$738,805	\$0.2132	\$49,011	\$105,208
	4.7	Grid-Gen-Bat-PV- WT2	20kW / 10kW	Region-1	15	10	27.3	76.8	—	—	—	29.8%	\$818,840	\$0.2402	\$54,961	\$108,331
	4.8	Grid-Gen-Bat-PV- WT1	20kW / 20kW	Region-2	15	9	28.2	79	—	—	—	32.8%	\$800,392	\$0.2336	\$53,397	\$110,103
	4.9	Grid-Gen-Bat-PV- WT1	20kW / 20kW	Region-1	15	8	25.1	66.2	1	—	—	38.3%	\$718,822	\$0.2071	\$47,657	\$102,733
	4.10	Grid-Gen-Bat-PV- WT2	20kW / 20kW	Region-2	15	9	27.3	68.2	1	—	—	38.3%	\$738,898	\$0.2117	\$48,893	\$106,830
	4.11	Grid-Gen-Bat-PV- WT2	20kW / 20kW	Region-1	15	10	27.3	76.8	—	—	—	29.8%	\$818,840	\$0.2402	\$54,961	\$108,331
	4.12	Grid-Gen-Bat-PV- WT1	20kW / 20kW	Region-2	15	9	28.2	79	—	—	—	32.8%	\$800,392	\$0.2336	\$53,397	\$110,103
	4.13	Grid-Gen-Bat-PV- WT1	35kW / 0kW	Region-1	—	3	23.4	54.8	1	—	—	34.9%	\$526,155	\$0.1558	\$34,484	\$80,359
	4.14	Grid-Gen-Bat-PV- WT2	35kW / 0kW	Region-2	—	3	25.8	60.1	1	—	—	35.1%	\$533,608	\$0.1580	\$34,574	\$86,648
	4.15	Grid-Gen-Bat-PV- WT2	35kW / 0kW	Region-1	—	3	26.4	67.8	—	—	—	27.8%	\$579,355	\$0.1716	\$38,081	\$87,061
	4.16	Grid-Gen-Bat-PV- WT1	35kW / 10kW	Region-2	—	3	27.2	69.6	—	—	—	29.1%	\$564,891	\$0.1673	\$37,328	\$82,336
	4.17	Grid-Gen-Bat-PV- WT1	35kW / 10kW	Region-1	—	3	24.4	57.1	1	—	—	36.8%	\$524,823	\$0.1522	\$34,171	\$83,080
	4.18	Grid-Gen-Bat-PV- WT2	35kW / 10kW	Region-2	—	3	26	59.9	1	—	—	36.5%	\$532,054	\$0.1540	\$34,455	\$86,639
	4.19	Grid-Gen-Bat-PV- WT2	35kW / 10kW	Region-1	—	3	26.8	67.1	—	—	—	28.2%	\$579,056	\$0.1706	\$38,080	\$86,778
	4.20	Grid-Gen-Bat-PV- WT1	35kW / 20kW	Region-2	—	3	27.3	67.3	—	—	—	30.7%	\$564,866	\$0.1660	\$36,939	\$87,332
4.21	Grid-Gen-Bat-PV- WT1	35kW / 20kW	Region-1	—	3	24.4	57.1	1	—	—	36.8%	\$524,822	\$0.1522	\$34,171	\$83,080	
4.22	Grid-Gen-Bat-PV- WT2	35kW / 20kW	Region-2	—	3	26.1	61.4	1	—	—	36.9%	\$532,019	\$0.1537	\$34,341	\$88,079	
4.23	Grid-Gen-Bat-PV- WT2	35kW / 20kW	Region-1	—	3	26.8	67.1	—	—	—	28.2%	\$579,056	\$0.1706	\$38,080	\$86,778	
4.24	Grid-Gen-Bat-PV- WT2	35kW / 20kW	Region-2	—	3	27.3	67.3	—	—	—	30.7%	\$564,866	\$0.1660	\$36,939	\$87,332	

TABLE 16. Simulation results of Scenario-4.

depicting the nominal situation: a 25% decrease in fuel cost, 25% increase in solar radiation, and 25% increase in wind speed.

When evaluating the results of Scenario-1, it was observed that only a 25% decrease in fuel cost affected the COE, whereas solar radiation and wind speed variations had no effect because they were not utilized. The effect of the fuel cost change was only 0.15% because the minimal use of the generator. Similarly, in Scenario-2, only the change in the fuel cost had a positive effect on the unit COE, with a decrease of 0.15%. By contrast, the sensitivity analysis for Scenario-3 indicated that the studied factors had a positive effect on the unit COE. The change in fuel cost had the highest effect at 17.34%, while the changes in solar radiation and wind speed had positive effect of 2.31% and 4.57%, respectively. Finally, for Scenario-4, the fuel cost changes did not affect the unit COE owing to the absence of generator usage. It was found that the change in solar radiation had a 3.48% positive effect and the change in wind speed had a 5.78% positive effect on COE.

Comparisons of renewable rates for Region-1 obtained from the sensitivity analysis, are presented in Figure 12. Because no RES were used in Scenario-1 and Scenario-2, the renewable rates remained constant at 0%. For Scenario-3, the sensitivity analyses showed that the change in fuel cost affected 2.0%, the change in solar radiation affected 0.6%, and the change in wind speed affected 3.8% of the renewable rate. In Scenario-4, the fuel cost changes did not affect the renewable rate owing to the absence of generator usage. However, the change in solar radiation affected 2.1% and the change in wind speed affected 2.9% of the renewable rate.

2) *General Evaluation for Region-2.* Figure 13 presents comparisons of the unit COE obtained for Region-2 as a result of the sensitivity analysis, specific to each scenario.

For each scenario, the bar graph form of nominal situation data, as well as the situations where fuel cost is reduced by 25%, solar radiation is increased by 25%, and wind speed is increased by 25%, are presented for comparison.

Regarding the results of Scenario-1, it was found that only a 25% decrease in the fuel cost affected the COE. Solar radiation and wind speed variations had no effect as these systems were not used. The effect of the fuel cost change was only 0.15% owing to the minimal use of the generator. Similarly, in Scenario-2, only the change in the fuel cost affected the unit COE. The effect was also positive, with a decrease of 0.15%. As the region did not differ between the results of Scenario-1 and Scenario-2, they yielded the same outcomes.

The results of Scenario-3 showed that the factors for which the sensitivity analysis was performed had a positive effect on the unit COE. The highest effect was achieved by the change in fuel cost (17.61%). The change in solar radiation affected the COE by 2.29%, whereas the change in wind speed had an effect of 4.01%. In Scenario-4, once again, it was shown that fuel cost changes would not affect the unit COE because of the absence of generator usage. However, it was observed that the change in solar radiation and wind speed affected the COE by 2.86% and 6.38%, respectively.

Comparisons of renewable rates for Region-2 obtained from the sensitivity analysis are presented in Figure 14. Because no RES were used in Scenario-1 and Scenario-2, the renewable rates remained constant at 0%. For Scenario-3, the sensitivity analyses showed that the change in fuel cost affected 1.0%, the change in solar radiation affected 0.9%, and the change in wind speed affected 2.8% on the renewable rate. In Scenario-4, the fuel cost changes did not affect the renewable rate owing to the absence of generator usage. The change in solar radiation affected 1.3% and the change in wind speed affected 4.3% of the renewable rate.

Upon comparison with the Region-1 results, it appears that the sensitivity analysis of parameter variations may

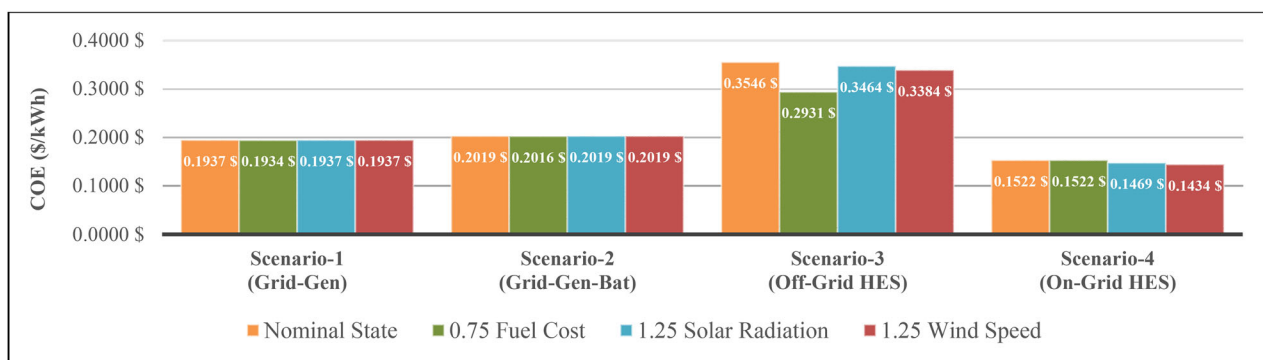


FIGURE 11. COE (\$/kWh) comparisons of sensitivity analyzes for Region-1 for the 4 main scenarios.

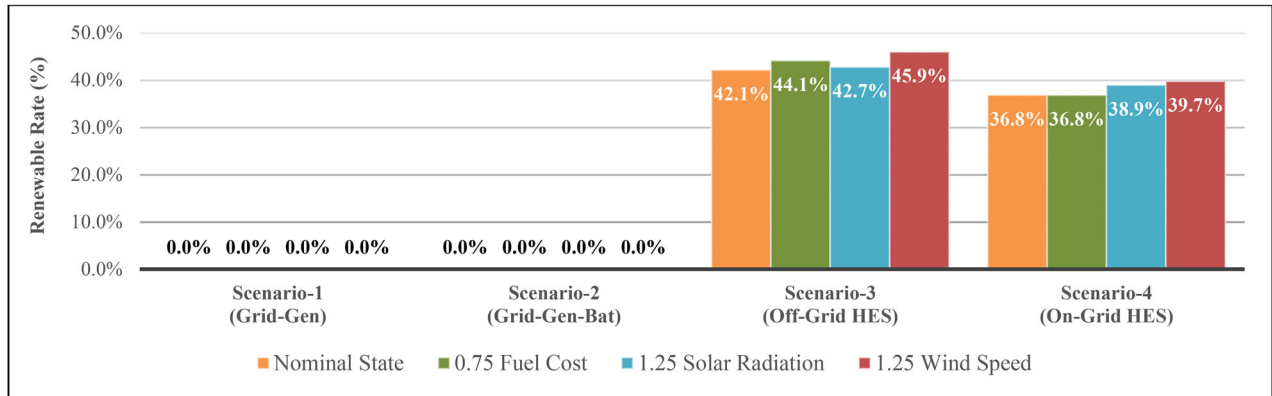


FIGURE 12. Renewable rate (%) comparisons of sensitivity analyzes for Region-1 for the 4 main scenarios.

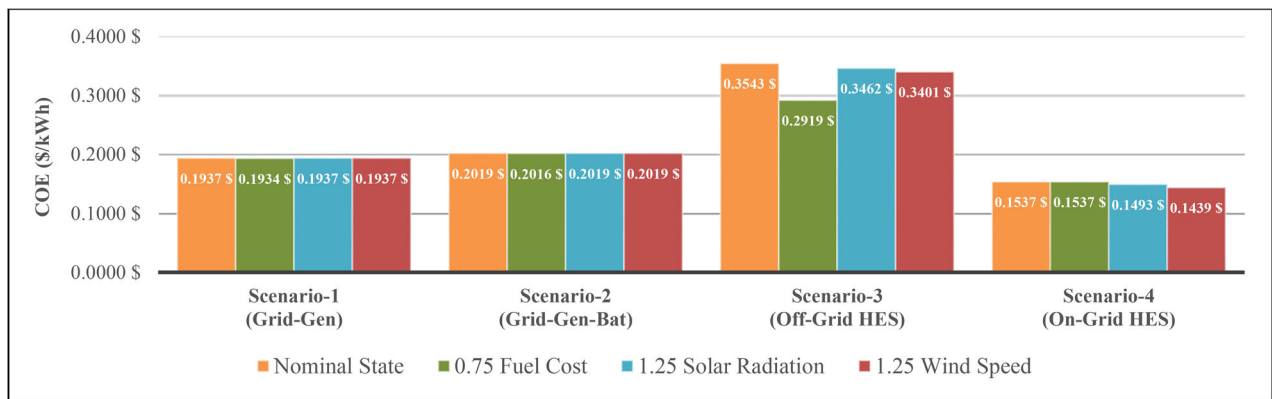


FIGURE 13. COE (\$/kWh) comparisons of sensitivity analyzes for Region-2 for the 4 main scenarios.

yield more favorable results for the on-grid HES solution in Scenario-4.

5. DISCUSSION OF RESULTS

In total, 31 different sub-case studies with varying resource options and grid limits were simulated for the four main scenarios. The optimum solutions were obtained separately for each scenario. After careful evaluation, the most suitable solutions were selected as follows:

- Scenario-1,
- Scenario-2.2, which is a subset of Scenario-2 with a 20kW generator usage limit,
- Scenario-3.1 and Scenario-3.2, created for the two study regions using the EO10 WT option in Scenario-3,
- Scenario-4.21 and Scenario-4.22, created for the two study regions with the EO10 WT option, 35kW grid purchase, and 20kW grid sales limit in Scenario-4,

Table 17 shows a comparison of all solutions obtained within each scenario, as well as comparisons by region.

For both Region-1 and Region-2, the solutions obtained under Scenario-3 and Scenario-4 had similar system component configurations. However, Region-2 has a higher solar radiation potential owing to its southern location, which leads to a relatively higher usage of PV panels. Furthermore, the Scenario-4 analysis revealed that the on-grid hybrid system solutions required less hardware than the off-grid systems presented in Scenario-3.

Figure 15 presents a comparison of the unit COE values for the optimum solutions obtained in the four main scenarios. A grid unit COE of 0.19 \$/kWh was used as the reference value. The Scenario-1 solution had a unit COE of 0.1937 \$/kWh, making it 2% more expensive than using the grid. In Scenario-2.2, which was determined to be the optimum solution for Scenario-2, the unit COE was calculated as 0.2019 \$/kWh, making it 6% more expensive than the grid unit COE.

The off-grid HES solutions exhibit the highest unit COE values. For Region-1 in Scenario-3, the unit COE for the optimum solution (Scenario-3.1) was 0.3546 \$/kWh, while for Region-2, the COE was 0.3543 \$/kWh in the optimum

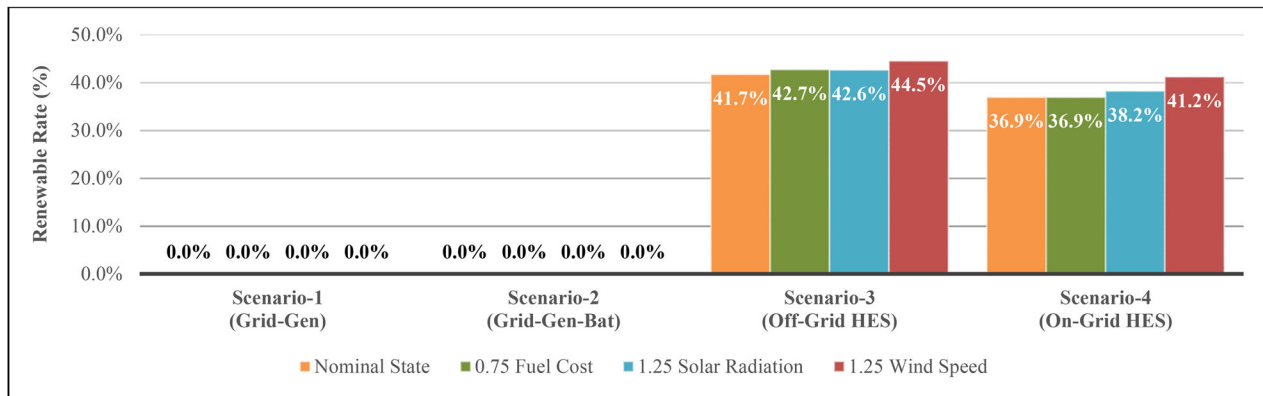


FIGURE 14. Renewable rate (%) comparisons of sensitivity analyzes for Region-2 for the 4 main scenarios.

solution (Scenario-3.2). Notably, the unit COE for Region-2 was relatively low, and the unit COEs calculated for both regions were 86-87% more expensive than the grid unit COE.

By contrast, the on-grid HES solutions had the lowest unit COEs. For Region-1 in Scenario-4, the unit COE for the optimum solution (Scenario-4.21) was 0.1522 \$/kWh, while for Region-2, the COE was 0.1537 \$/kWh in the optimum solution (Scenario-4.22). It is worth noting that the unit COE calculated for Region-1 was relatively lower. Furthermore, because no generator usage was proposed in the optimum solutions, more environmentally friendly and 19-20% more economical results were obtained compared to the grid unit COE in comparison to other scenarios.

Figure 16 presents a comparison of the renewable rate values calculated for the optimum solutions obtained in the four main scenarios. The renewable rate is zero for Scenario-1 and Scenario-2 because no RES is utilized. Among the off-grid solutions in Scenario-3, the highest renewable rate of 42% was achieved, which can be attributed to the high generator usage. By contrast, Scenario-4, which represents an on-grid HES, achieved a renewable rate of 37%. This is close to the renewable rate achieved in the off-grid HES solutions in Scenario-3.

The annual fuel consumption values (L/year) obtained from the optimum solutions for the four main scenarios are shown in Figure 17. The fuel consumption in Scenario-1 is expected to be 275 L/year, whereas it is 236 L/year in Scenario-2. It was observed that the battery support in Scenario-2 can reduce fuel consumption by 15% compared to the Scenario-1 solution.

On average, the annual fuel consumption of the solutions in Scenario-3 was 47,700 L/year. It is evident that this off-grid solution has high generator usage, resulting in significantly higher fuel consumption than the Scenario-1 solution. In Scenario-4, where there was no generator usage, no fuel consumption was observed.

The comparative CO and CO₂ emission values (kg/year) obtained from the optimum solutions for the four main scenarios are presented in Figures 18 and 19. In Scenario-1 and Scenario-2, CO emissions were negligible owing to low generator usage. Conversely, the high generator usage in Scenario-3 results in significantly higher CO emissions. However, CO emissions are not anticipated in Scenario-4 since no generator usage is involved. When comparing the CO₂ emission values, the highest emissions were observed in Scenario-1 and Scenario-2 solutions, while the lowest CO₂ emission value was obtained in the solutions of Scenario-4. Compared to Scenario-1 and Scenario-2 solutions, Scenario-3 solutions demonstrate approximately 25% less CO₂ emission, whereas Scenario-4 solutions offer approximately 35% less CO₂ emission. Therefore, the most environmentally friendly solution was the on-grid HES in Scenario-4.

In addition, along with the sensitivity analyses, it can be observed that the on-grid HES solutions in Scenario-4 are the most cost-effective solution. Although off-grid HES solutions appear to have a higher renewable rate, on-grid HES solutions have a significantly higher renewable rate which cannot be ignored. Positive changes in solar radiation and wind speed could have a positive impact on the optimal solutions in Scenario-4.

6. CONCLUSION

Ensuring uninterrupted operation of security systems is essential for the safety of critical infrastructure, particularly in seaports. Thus, meeting the energy requirements of security systems without interruption is of utmost importance. This study aims to analyze the optimal design of a hybrid energy system (HES) for security systems in two different climatic regions of Türkiye: Samsun Seaport (Region-1) and

Case	Energy resource options	Grid purchase /Sale limits	Gen. usage upper limit	Region	System component size							System costs			
					Gen. (kW)	Bat. (UNIT)	CT (kW)	PV (kW)	WT1 (UNIT)	WT2 (UNIT)	NPC -25 Yrs- (\$)	COE (\$/kWh)	O&M (\$/yr)	IC (\$)	
1	Grid-Gen-	No Limit / 0 kW	No Limit	Region-1 & Region-2	25	—	—	—	—	—	—	\$654,305	\$0.1937	\$49,646	\$12,500
2.2	Grid-Gen-Bat-	No Limit / 0 kW	20kW	Region-1 & Region-2	35	19	31.6	124	1	—	—	\$681,475	\$0.2019	\$50,519	\$28,388
3.1	Gen-Bat-	—	No Limit	Region-1	35	19	31.6	124	1	—	—	\$1,198,083	\$0.3546	\$79,084	\$175,720
3.2	PV- WT1	—	No Limit	Region-2	35	22	31.6	127	1	—	—	\$1,197,034	\$0.3543	\$78,645	\$180,350
4.21	Grid-Gen- Bat-	35kW / 20kW	No Limit	Region-1	—	3	24.4	57.1	1	—	—	\$524,822	\$0.1522	\$34,171	\$83,080
4.22	PV- WT1	35kW / 20kW	No Limit	Region-2	—	3	26.1	61.4	1	—	—	\$532,019	\$0.1537	\$34,341	\$88,079

TABLE 17. Comparison of optimum solutions for 4 main scenarios.

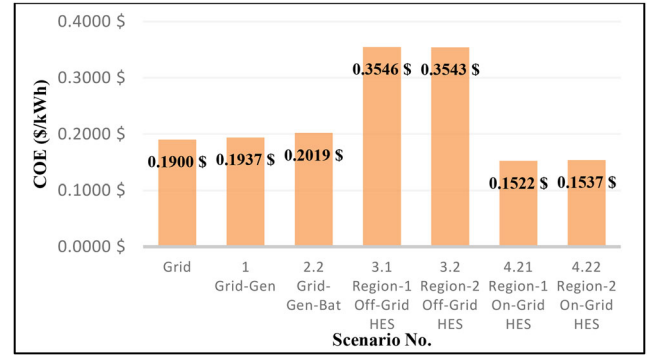


FIGURE 15. COE (\$/kWh) comparisons of the optimum solutions obtained for the 4 main scenarios.

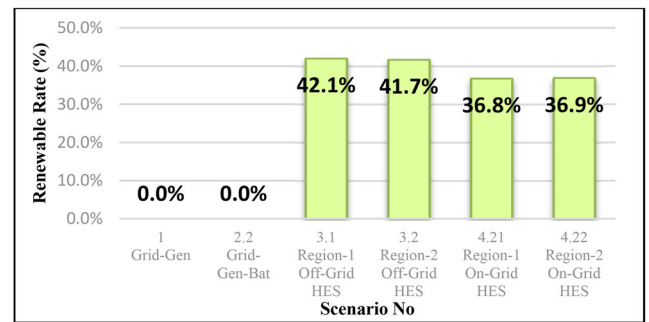


FIGURE 16. Renewable rate comparisons of the optimum solutions obtained for the 4 main scenarios.

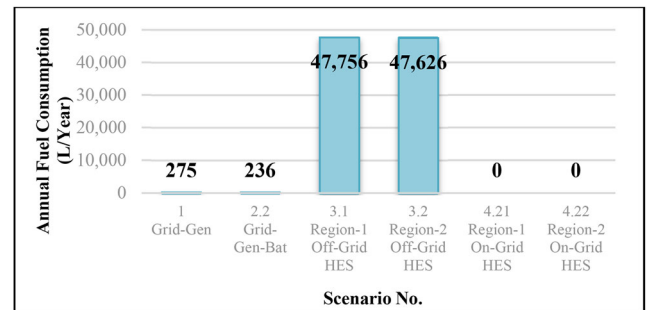


FIGURE 17. Annual fuel consumption (L/year) comparisons of the optimum solutions obtained for the 4 main scenarios.

Antalya Seaport (Region-2). The study investigates various energy sources to supply the system, compares HES solutions with conventional options such as generators and batteries, and examines regional variations in the results.

This study encompasses 31 sub-scenarios derived from four main scenarios, considering security system load profiles, resource options, grid limitations, wind turbine alternatives, and constraints. Comprehensive and comparative analyses were conducted using HOMER software to identify the most

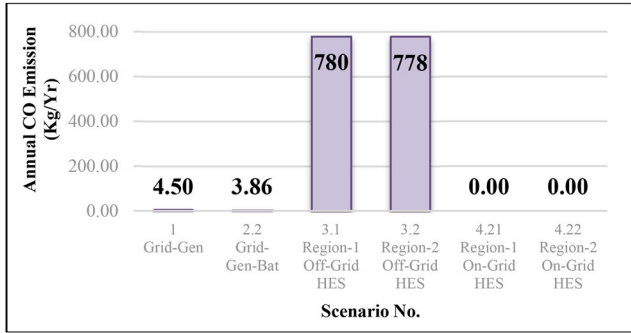


FIGURE 18. Annual CO emission (kg/year) comparisons of the optimum solutions obtained under the 4 main scenarios.

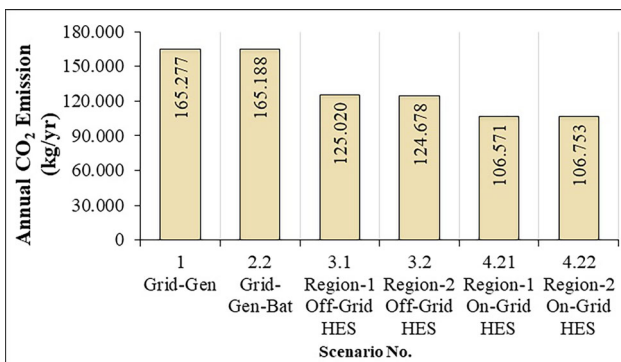


FIGURE 19. Annual CO₂ emission (kg/year) comparisons of the optimum solutions obtained for the 4 main scenarios.

suitable technical, economic, and environmental solutions. The objective was to obtain optimal solutions with a unit cost below the grid unit cost for a service life of 25 years.

Six optimal energy system solutions are presented for each region. The results demonstrate that on-grid HES solutions are more economical and environmentally friendly compared to conventional generator-battery or off-grid HES solutions. On-grid HES solutions exhibited a cost advantage of 19–20% below the grid unit cost while eliminating the need for generators, leading to a greener outcome.

Sensitivity analysis revealed that off-grid HES solutions were significantly disadvantaged in terms of levelized cost of electricity (COE) and carbon emissions. On-grid HES solutions proved to be the most favorable in terms of unit COE, CO, and CO₂ emissions in both regions. Overall, the study demonstrated that HES solutions can provide a 25-year service life while delivering reliable power to security systems. These findings indicate a growing demand for HES solutions in the future, driven by potential advancements in renewable energy sources and energy storage units, leading to improved efficiency and cost reductions.

In future studies, it is envisioned to expand this research to different regions, considering various energy storage systems and more efficient photovoltaic-wind turbine (PV-WT) combinations. Additionally, similar optimization studies for critical buildings such as hospitals, military facilities, and administrative buildings will be evaluated.

DISCLOSURE STATEMENT

No potential conflict of interest was reported by the authors.

REFERENCES

- [1] N. A. B. A. Razak, M. M. Bin Othman and I. Musirin, "Optimal sizing and operational strategy of hybrid renewable energy system using HOMER," presented at the PEOCO 2010 - 4th Int. Power Eng. Optim. Conf. Progr. Abstr., 2010, pp. 495–501. DOI: [10.1109/PEOCO.2010.5559240](https://doi.org/10.1109/PEOCO.2010.5559240).
- [2] B. E. Turkyay and A. Y. Telli, "Economic analysis of stand-alone and grid connected hybrid energy systems," *Renew. Energy*, vol. 36, no. 7, pp. 1931–1943, Jul. 2011. DOI: [10.1016/j.renene.2010.12.007](https://doi.org/10.1016/j.renene.2010.12.007).
- [3] A. Sharma, A. Singh and M. Khemariya, "Homer optimization based solar PV; wind energy and diesel generator based hybrid system," *Int. J. Soft Comput. Eng. (IJSCE)*, vol. 3, no. 1, pp. 199–204, 2013.
- [4] Z. Iverson, A. Achuthan, P. Marzocca and D. Aidun, "Optimal design of hybrid renewable energy systems (HRES) using hydrogen storage technology for data center applications," *Renew. Energy*, vol. 52, pp. 79–87, 2013. DOI: [10.1016/j.renene.2012.10.038](https://doi.org/10.1016/j.renene.2012.10.038).
- [5] K. E. Okedu and R. Uhumwango, "Optimization of renewable energy efficiency using HOMER," *Int. J. Renew. Energy Res.*, vol. 4, no. 2, pp. 421–427, 2014.
- [6] U. S. Magarappanavar and S. Koti, "Optimization of wind-solar-diesel generator hybrid power system using HOMER," *Int. Res. J. Eng. Technol. (IRJET)*, vol. 3, no. 06, pp. 522–526, 2016.
- [7] M. Baneshi and F. Hadianfard, "Techno-economic feasibility of hybrid diesel/PV/wind/battery electricity generation systems for non-residential large electricity consumers under southern Iran climate conditions," *Energy Convers. Manag.*, vol. 127, pp. 233–244, 2016. DOI: [10.1016/j.enconman.2016.09.008](https://doi.org/10.1016/j.enconman.2016.09.008).
- [8] N. M. Swarnkar, L. Gidwani and R. Sharma, "An application of HOMER Pro in optimization of hybrid energy system for electrification of technical institute," presented at the 2016 Int. Conf. Energy Effic. Technol. Sustain. ICEETS 2016, pp. 56–61. Oct., 2016. DOI: [10.1109/ICEETS.2016.7582899](https://doi.org/10.1109/ICEETS.2016.7582899).
- [9] M. Nurunnabi and N. K. Roy, "Grid connected hybrid power system design using HOMER," presented at the Proc. 2015 3rd Int. Conf. Adv. Electr. Eng. ICAEE 2015, pp. 18–21. Jul., 2016. DOI: [10.1109/ICAEE.2015.7506786](https://doi.org/10.1109/ICAEE.2015.7506786).

- [10] P. Kumar, R. Pukale, N. Kumabhar and U. Patil, "Optimal design configuration using HOMER," *Procedia Technol.*, vol. 24, pp. 499–504, 2016. DOI: [10.1016/j.protcy.2016.05.085](https://doi.org/10.1016/j.protcy.2016.05.085).
- [11] S. Bahramara, M. P. Moghaddam and M. R. Haghifam, "Optimal planning of hybrid renewable energy systems using HOMER: a review," *Renew. Sustain. Energy Rev.*, vol. 62, pp. 609–620, 2016. DOI: [10.1016/j.rser.2016.05.039](https://doi.org/10.1016/j.rser.2016.05.039).
- [12] L. M. Halabi, S. Mekhilef, L. Olatomiwa and J. Hazelton, "Performance analysis of hybrid PV/diesel/battery system using HOMER: a case study Sabah, Malaysia," *Energy Convers. Manag.*, vol. 144, pp. 322–339, 2017. DOI: [10.1016/j.enconman.2017.04.070](https://doi.org/10.1016/j.enconman.2017.04.070).
- [13] A. A. Mas'ud, "The Application of Homer Optimization Software to Investigate the Prospects of Hybrid Renewable Energy System in Rural Communities of Sokoto in," *Int. J. Electr. Comput. Eng. Int. J. Electr. Comput. Eng. Int. J. Electr. Comput. Eng.*, vol. 7, no. 2, pp. 596–603, 2017. DOI: [10.11591/ijece.v7i2.pp596-603](https://doi.org/10.11591/ijece.v7i2.pp596-603).
- [14] A. Jamalalah, C. P. Raju and R. Srinivasarao, "Optimization and operation of a renewable energy based pv-fc-micro grid using homer," presented at the Proc. Int. Conf. Inven. Commun. Comput. Technol. ICICCT 2017, pp. 450–455. Jul., 2017. DOI: [10.1109/ICICCT.2017.7975238](https://doi.org/10.1109/ICICCT.2017.7975238).
- [15] M. Tesfaye Yeshalem, B. Khan and M. T. Yeshalem, "Design of an off-grid hybrid PV/wind power system for remote mobile base station: a case study Distribution System Reliability Improvement with DG and Optimal Placement of Protection Devices View project Call for paper for a Special Issue in the "Frontier," 2017. DOI: [10.3934/energy.2017.1.96](https://doi.org/10.3934/energy.2017.1.96).
- [16] L. Grange, G. Da Costa and P. Stolf, "Green IT scheduling for data center powered with renewable energy," *Futur. Gener. Comput. Syst.*, vol. 86, pp. 99–120, 2018. DOI: [10.1016/j.future.2018.03.049](https://doi.org/10.1016/j.future.2018.03.049).
- [17] M. Nurunnabi, N. K. Roy, E. Hossain and H. R. Pota, "Size optimization and sensitivity analysis of hybrid wind/PV micro-grids- A case study for Bangladesh," *IEEE Access*, vol. 7, pp. 150120–150140, 2019. DOI: [10.1109/ACCESS.2019.2945937](https://doi.org/10.1109/ACCESS.2019.2945937).
- [18] F. S. Azad, I. Ahmed, S. R. Hossain and R. Amin Tuhin, "HOMER optimized off-grid hybrid energy system: a case study on rohingya relocation center in Bangladesh," presented at the 1st Int. Conf. Adv. Sci. Eng. Robot. Technol. 2019, ICASERT 2019, May, 2019. DOI: [10.1109/ICASERT.2019.8934534](https://doi.org/10.1109/ICASERT.2019.8934534).
- [19] İ. Çetinbaş, B. Tamyürek and M. Dermitas, "Design, analysis and optimization of a hybrid microgrid system using HOMER software: eskisehir Osmangazi University example," *IJRED*, vol. 8, no. 1, pp. 65–79, Feb. 2019. DOI: [10.14710/ijred.8.1.65-79](https://doi.org/10.14710/ijred.8.1.65-79).
- [20] M. Usman, A. M. Malik, A. Mahmood, A. Kousar and K. Sabeel, "HOMER analysis for integrating solar energy in off-grid and on-grid SCO telecommunication sites," presented at the Proc. - 2019 IEEE 1st Glob. Power, Energy Commun. Conf. GPECOM 2019, pp. 270–275. Jun., 2019. DOI: [10.1109/GPECOM.2019.8778511](https://doi.org/10.1109/GPECOM.2019.8778511).
- [21] L. Khalil, K. Liaquat Bhatti, M. Arslan Iqbal Awan, M. Riaz, K. Khalil and N. Alwaz, "Optimization and designing of hybrid power system using HOMER pro," *Mater. Today Proc.*, vol. 47, pp. S110–S115, 2021. DOI: [10.1016/j.matpr.2020.06.054](https://doi.org/10.1016/j.matpr.2020.06.054).
- [22] S. Kwon, "Ensuring renewable energy utilization with quality of service guarantee for energy-efficient data center operations," *Appl. Energy*, vol. 276, no. July, pp. 115424, 2020. DOI: [10.1016/j.apenergy.2020.115424](https://doi.org/10.1016/j.apenergy.2020.115424).
- [23] T. MuthuKumaran, P. A. D. V. Raj, K. Murugaperumal and N. P. Subramanian, "Feasibility Analysis of PV/Wind/DG Based Hybrid Energy System Design for Indian Educational Institute," presented at the 3rd IEEE Int. Virtual Conf. Innov. Power Adv. Comput. Technol. i-PACT 2021, 2021. DOI: [10.1109/I-PACT52855.2021.9696911](https://doi.org/10.1109/I-PACT52855.2021.9696911).
- [24] M. Purlu, S. Beyarslan and B. E. Turkay, "Optimal design of hybrid grid-connected microgrid with renewable energy and storage in a rural area in turkey by using HOMER," presented at the 2021 13th Int. Conf. Electr. Electron. Eng. ELECO 2021, pp. 263–267., 2021. DOI: [10.23919/ELECO54474.2021.9677788](https://doi.org/10.23919/ELECO54474.2021.9677788).
- [25] Y. Sawle, S. Jain, S. Babu, A. R. Nair and B. Khan, "Prefeasibility economic and sensitivity assessment of hybrid renewable energy system," *IEEE Access*, vol. 9, pp. 28260–28271, 2021. DOI: [10.1109/ACCESS.2021.3058517](https://doi.org/10.1109/ACCESS.2021.3058517).
- [26] L. Uwineza, H. G. Kim and C. K. Kim, "Feasibility study of integrating the renewable energy system in Popova Island using the Monte Carlo model and HOMER," *Energy Strateg. Rev.*, vol. 33, pp. 100607, Jan. 2021. DOI: [10.1016/j.esr.2020.100607](https://doi.org/10.1016/j.esr.2020.100607).
- [27] K. K. Sharma, et al., "Economic evaluation of a hybrid renewable energy system (HRES) using hybrid optimization model for electric renewable (HOMER) software-a case study of rural India," *Int. J. Low-Carbon*, vol. 16, no. 3, pp. 814–821, 2021. DOI: [10.1093/ijlct/ctab012](https://doi.org/10.1093/ijlct/ctab012).
- [28] M. A. Kabir, S. Hossain, M. S. Islam, M. M. H. Imran, M. R. Akhanjee and A. Hossain, "Energy consumption analysis of a hybrid optimized model for sustainable green data center," presented at the 2021 Int. Conf. Sci. Contemp. Technol. ICSCCT 2021, 2021. DOI: [10.1109/ICSCCT53883.2021.9642599](https://doi.org/10.1109/ICSCCT53883.2021.9642599).
- [29] R. B. Sitanggang, "Study of a hybrid system with various types of energy storage in Wetar Island," presented at the IES 2022 - 2022 Int. Electron. Symp. Energy Dev. Clim. Chang. Solut. Clean Energy Transition, Proceeding, pp. 104–109., 2022. DOI: [10.1109/IES55876.2022.9888271](https://doi.org/10.1109/IES55876.2022.9888271).
- [30] A. Sawhney, S. Bracco, F. Delfino and B. Bonvini, "Optimal planning and operation of a small size Microgrid within a Positive Energy District," presented at the 2022 AEIT Int. Annu. Conf. AEIT 2022, 2022. DOI: [10.23919/AEIT56783.2022.9951718](https://doi.org/10.23919/AEIT56783.2022.9951718).
- [31] A. Al Badi and A. Al Wahaibi, "Techno-economic analysis and optimization of solar energy system for power generation and hydrogen production in Al Mazyouna Area," presented at the 2022 3rd Int. Conf. Clean Green Energy Eng., pp. 26–31. Aug., 2022. DOI: [10.1109/CGEE55282.2022.9976768](https://doi.org/10.1109/CGEE55282.2022.9976768).

- [32] URL-12, "Meteoroloji Genel Mudurlugu/Turkiye Gunes Radyasyonu Haritası." https://www.mgm.gov.tr/kurumici/radyasyon_iller.aspx, date. Accessed November 2022.
- [33] URL-13, "Meteoroloji Genel Mudurlugu/Turkiye Ruzgâr Atlası." <https://www.mgm.gov.tr/genel/ruzgar-atlasi.aspx>, date. Accessed November 2022.
- [34] URL-15, "Wikipedia/2015 Turkiye Blackout." https://en.wikipedia.org/wiki/2015_Turkey_blackout, date. Accessed October 2022.

BIOGRAPHIES

Mahmut Hudayi Kiyak was born in Samsun, Turkiye. He received the B.S. degree in electrical engineering from Yildiz Technical University, Istanbul, Turkiye, in 2019. He has been pursuing his M.S degree in electrical engineering at Istanbul Technical University (ITU) since 2020. Since 2019, he has been working as a System Design Engineer at ASELSAN Inc., in Ankara, Turkiye. His research interests include security systems, renewable energy systems, system optimization, power systems, electric vehicles, and wireless power transfer systems.

Mikail Purlu was born in Sivas, Turkiye. He received the B.S. degree in electrical and electronics engineering from Sivas Cumhuriyet University, Sivas, Turkiye, in 2013, the M.S. degree in electrical engineering from Istanbul Technical University (ITU), Istanbul, Turkiye, in 2017, and the Ph.D. degree in electrical engineering from ITU, Istanbul, Turkey, in 2022. Between 2014 and 2022, he worked as a Research Assistant at ITU. Since 2023, he has

been working as an Assist. Prof. at Sivas Cumhuriyet University. He is a member of CIGRE Turkiye and a Technical Writer Editor of the Turkish Journal of Electrical Power and Energy Systems (TEPES). His research interests include distributed generation, optimization of power systems, renewable energy, and smart grids.

Belgin Emre Turkay was born in Istanbul, Turkiye. She received the B.S., M.S., and Ph.D. degrees in electrical engineering from Istanbul Technical University (ITU), Istanbul. She is currently a Professor and the Head of the Department of Electrical Engineering, ITU. She is a member of CIGRE Turkiye and an Editor of the Turkish Journal of Electrical Power and Energy Systems (TEPES). Her research interests include power quality, renewable energy, smart grids, and power system resilience.

Tahir Cetin Akinci (Senior Member IEEE) pursued his Bachelor's degree in Electrical Engineering in 2000, followed by his Master's and Ph.D. degrees in 2005 and 2010, respectively. From 2003 to 2010, he worked as a Research Assistant at Marmara University in Istanbul, Turkey. Dr. Akinci is currently a full professor in the Electrical Engineering Department at Istanbul Technical University (ITU) in 2020. Dr. Akinci assumed the role of a visiting scholar at the University of California Riverside (UCR). His research interests including power systems, artificial neural networks, deep learning, machine learning, cognitive systems, signal processing, and data analysis.